

Optical signatures of electron correlations in the cuprates

Lecture notes

Invited talk at the Trieste miniworkshop "Strong Correlation in the high Tc era"

17-28 July 2000, ICTP, Trieste, Italy.

D. van der Marel (*presenting author*)

H. J. Molegraaf, C. Presura, M.-U Grueninge, B. Dam*

Laboratory of Solid State Physics of the Materials Science Centre, University of Groningen, Nijenborgh 4, 9747 AG Groningen, The Netherlands

* *Vrije Universiteit Amsterdam*

(8 may - 14 july 2000)

We discuss optical techniques to measure changes in kinetic energy and Coulomb energy associated with the superconducting state. The changes of correlation energy due to d-wave and s-wave superconducting correlations are discussed quantitatively, in momentum space and in direct space. The correlation functions are demonstrated to be remarkably different for s- and d-wave pairing, demonstrating rather directly that quite different s- and d-wave pairing are stabilized by qualitatively different mechanism. The direction of change of kinetic energy is discussed, both for conventional BCS superconductivity and for recent proposals based on non-Fermi liquid approaches. Experimental results are shown for YBCO, which prove that the correlation energy *increases* in the long wavelength limit when the system enters the superconducting state. We review the experiments aimed at determining the change of kinetic energy along the c-direction. In some cases, in particular the underdoped cuprates, there is evidence for some decrease along the c-direction, but the energy change is orders of magnitude lower than the condensation energy. The relative changes of the in-plane low frequency spectral weight are of the order of 0.1 %. We introduce an experimental technique based on ellipsometric spectroscopy to measure these changes, which are related to the in-plane kinetic energy. With this novel method we are able to show for optimally doped YBCO, that the change of kinetic energy due to superconductivity is in the interval $-0.2meV < \delta E_{kin} < 0.03meV$ per unit cell.

I. INTRODUCTION

A necessary condition for the existence of superconductivity is, that the free energy of the superconducting state is lower than that of the non-superconducting state. At sufficiently high temperature important contributions to the free energy are due to the entropy. These contributions depend strongly on the nature of the low energy excitations, first and foremost of all their nature be it fermionic, bosonic or of a more complex character due to electron correlation effects. Since at $T = 0$ the entropy plays no role, the free energy is just the quantum mechanical expectation value of the total energy of the system, which can be separated in a kinetic energy contribution and a Coulomb correlation contribution.

A. The Coulomb Correlation energy

In a series of papers Leggett has discussed the change of Coulomb correlation energy for a system which becomes superconducting [1], and has argued, that this energy would actually decrease in the superconducting state. In this section we review the main results, while restricting the analysis to the following cases for the sake of simplicity:

- Only one superconducting layer per unit cell

- Free electron behaviour along the planes

- Superconducting δ -layers, with corresponding structure factor along c

We consider a system of electrons interacting via the Coulomb interaction

$$H = H_{kin} + \frac{1}{2} \int d^3\vec{r} \int \hat{n}(\vec{r}) V(\vec{r}, \vec{r}') \hat{n}(\vec{r}') d^3\vec{r}' \quad (1)$$

where V is the volume of the system and $V(\vec{r}, \vec{r}')$ is the screened Coulomb interaction

$$V(\vec{r}, \vec{r}') = \frac{e^2}{\epsilon_{sc} |\vec{r} - \vec{r}'|} \quad (2)$$

The factor ϵ_{sc} in the denominator is a real positive frequency independent number representing the screening of the Coulomb interaction by the polarizable ions. In the ground state of the system, the correlation function is just the quantum-expectation value of the last term of 1. This factors out as a product over all space coordinates of the interaction potential with the correlation function

$$v_c = \int \int V(\vec{r}, \vec{r}') g(\vec{r}, \vec{r}') d^3r' d^3r \quad (3)$$

The k-space representation of the correlation function is

$$g_k = \langle \Psi_0 | \hat{\rho}_k \hat{\rho}_{-k} | \Psi_0 \rangle \quad (4)$$

where the operator

$$\hat{\rho}_k = \sum_{p\sigma} c_{p+k\sigma}^\dagger c_{p\sigma} \quad (5)$$

is the Fourier transform of the particle density operator $\hat{n}(\vec{r})$. We define the interaction V_k as the projection of $V(r, r')$ on the electronic state vectors. With these definitions we see, that expression for the correlation energy becomes a quite simple one in the k -space representation

$$v_c = \sum_k V_k g_k \quad (6)$$

B. Dielectric constant and static structure factor

The dielectric constant is the ratio between the electric field of an externally oscillating test charge, and the induced field in a solid. The experimentally determined dielectric constant using optical spectroscopy or EELS is $\epsilon(\vec{k}, \omega)$. We are interested in the dielectric constant due to the charge carriers in the system. We therefor treat the field of the test charge screened by the ion cores as an effective 'external' field. The effective dielectric constant is then $\tilde{\epsilon}(\vec{k}, \omega) = \epsilon(\vec{k}, \omega)/\epsilon_b$, where ϵ_b takes into account the screening of external fields by the ion cores. It was shown by Nozieres and Pines [2], that the dielectric constant satisfies

$$\text{Im} \left(\frac{1}{\tilde{\epsilon}(\vec{k}, \omega)} \right) = -\frac{\pi V_{\vec{k}}}{\hbar} \sum_{\nu} (\rho_{\vec{k}}^{\nu})^2 \delta(\omega_{\nu 0} - \omega) \quad (7)$$

for the system in it's groundstate Ψ_0 .

$(\rho_{\vec{k}}^{\nu})_{\nu 0} = \langle \Psi_0 | \hat{\rho}_{\vec{k}} | \Psi_{\nu} \rangle$ is the matrix element of the density fluctuation between the ground-state wavefunction Ψ_0 and the excited state Ψ_{ν} , and $\hbar\omega_{\nu 0} = E_{\nu} - E_0$ is the energy difference between these two states. [3]

Integration of Eq. 7 leads to a remarkably useful relation between the dielectric function and the Fourier transform of van Hove's pair correlation function

$$-\frac{1}{\pi} \int_0^{\infty} \text{Im} \left[\frac{\hbar}{\tilde{\epsilon}(\vec{k}, \omega)} \right] d\omega = V_{\vec{k}} \langle \Psi_0 | \hat{\rho}_{\vec{k}} \hat{\rho}_{-\vec{k}} | \Psi_0 \rangle \quad (8)$$

After carrying out the Fouriertransform relating $\hat{\rho}_{\vec{k}}$ to $\hat{n}(\vec{r})$ and comparison with the interaction term of the Hamiltonian completes the proof that the Coulomb correlation energy per unit volume v_c follows from the knowledge of the dielectric constant $\epsilon(\vec{k}, \omega)$:

$$v_c + v_0 = \frac{\hbar}{(2\pi)^4} \int d^3\vec{k} \int_0^{\infty} \text{Im} \left[\frac{-1}{\tilde{\epsilon}(\vec{k}, \omega)} \right] d\omega \quad (9)$$

The second term on the left side of Eq. 9 corresponds to the interaction between static density fluctuations in the solid. This term is independent of the correlations present in the many-electron wave function, and it will be ignored in the subsequent discussion.

C. Correlation energy in layered electron gas

A Layered Electron gas is characterized by

1. (Quantum) confinement of the charge carriers to two dimensional layers
2. Absence of charge transport between the layers
3. Presence of three dimensional Coulomb interactions: The intra-plane and inter-plane interactions are finite.

As a result of the absence of charge transport, the pair-correlation function $\langle \Psi_0 | \hat{\rho}_k^j \hat{\rho}_{-k}^{j'} | \Psi_0 \rangle$ is zero for $j \neq j'$, except if $k = 0$. Here j and j' are the layer indices. In this subsection we use k and q to indicate the momentum quantum number parallel and perpendicular to the planes respectively. The only correlations of the ground-state wavefunction are therefor between density fluctuations within the same plane, *i.e.* those with $j = j'$.

In subsection II A we will demonstrate, that optical spectroscopy can be used to measure the small momentum sector of the Coulomb correlation energy. Strictly speaking the experiment provides directly the quantity $V_{k,q} \langle \Psi_0 | \hat{\rho}_{k,q} \hat{\rho}_{-k,-q} | \Psi_0 \rangle$ in the limit $k, q \rightarrow 0$. However, a more interesting quantity is $V_{k,j,j} \langle \Psi_0 | \hat{\rho}_k^j \hat{\rho}_{-k}^j | \Psi_0 \rangle$ involving only fluctuations within the *same* plane. Interestingly this quantity can also be calculated also from the the optical data, provided that the condition of absence of interlayer transport is satisfied.

The dielectric constant can quite generally be written in the form

$$\tilde{\epsilon}(k, q, \omega) = 1 - V(q, k) \left(\tilde{q}^2 \Pi'_{\parallel} + \tilde{k}^2 \Pi'_c \right) \quad (10)$$

where $\tilde{q}^2 = 2(\cosh(sq) - 1)/s^2$, and $\tilde{k}^2 = 2(1 - \cos(sk))/s^2$. Both Π'_{\parallel} and Π'_c are functions of q, k , and ω . However, in the limit $k, q \rightarrow 0$ both Π'_{\parallel} and Π'_c become finite constants. The above form is suggested by the RPA and Π' is closely related -but not identical- to the bare polarization bubble. The above form should be regarded as a *definition* of Π'_{\parallel} and Π'_c . In a layered electron system there is no electron transport along c perpendicular to the layers, even though the Coulomb forces are 3 dimensional (causing a finite dispersion of the dielectric function along c). The absence of transport *does* however imply that $\Pi'_c = 0$. Here we neglected the finite but small value of Π'_c which is responsible for the appearance of *e.g.* the c -axis Josephson plasmon in the high T_c cuprates. With optical spectroscopy we determine $\tilde{\epsilon}(\omega)$ at $k = 0$, either for electric fields along the plane (respectively $\epsilon_{\parallel}(\omega)$ and $\epsilon_c(\omega)$). In a layered electron gas with lattice constant s along the c -direction the Fourier transform of the Coulomb energy corresponds to a discrete lattice sum perpendicular to the planes, and a continuous 2D integral along the planes [4], providing

$$V(k, q) = \frac{4\pi e^2}{V} \frac{(s/2k) \sinh(ks)}{\cosh(ks) - \cos(qs)} \quad (11)$$

where V is the volume of the system. Taking Eq. 10 in the limit of small q , we observe that it can be conveniently written in the form

$$\tilde{\epsilon}(k, q, \omega) = 1 + \frac{(ks/2) \sinh(ks)}{\cosh(ks) - \cos(qs)} (\tilde{\epsilon}_{\parallel}(k, \omega) - 1) \quad (12)$$

With the help of this formula the expression for Coulomb correlation energy of the j 'th layer of a LEG can be expressed exclusively in terms of the *in-plane* polarizability $\alpha(k, \omega) = \epsilon_{\parallel}(k, \omega)/\epsilon_b - 1$, which for $k \rightarrow 0$ can be measured using optical spectroscopy. The integration over qs can be carried out quite easily using a simple contour integral over the unit circle, yielding [5]

$$v_c^j = \frac{\hbar}{(2\pi)^3} \int d^2\vec{k} \int_0^\infty d\omega \text{Im} \frac{|\vec{k}| \alpha(k, \omega)}{\sqrt{[1 + \frac{ks}{2} \tanh(\frac{ks}{2}) \alpha(k, \omega)][1 + \frac{ks}{2} / \tanh(\frac{ks}{2}) \alpha(k, \omega)]}} \quad (13)$$

We will distinguish two limiting cases. First, for $k_m s \gg 1$ in the denominator of the integrand we obtain [5] Eq. 4.5.1 of Ref. [1]

$$v_c^j = \frac{2}{s} \frac{\hbar}{(2\pi)^3} \int d^2\vec{k} \int_0^\infty d\omega \text{Im} \frac{-1}{1 + \frac{ks}{2} \left(\frac{\epsilon_{\parallel}(k, \omega)}{\epsilon_b} - 1 \right)} \quad (14)$$

Second, for small in-plane momentum limit $k_m s \ll 1$ we obtain

$$v_c^j = \hbar \left(\frac{k_m}{4\pi} \right)^3 \int_0^\infty d\omega \text{Im} \left\{ \sqrt{\epsilon_{\parallel}(\omega)/\epsilon_b} - \sqrt{\epsilon_b/\epsilon_{\parallel}(\omega)} \right\} d\omega \quad (15)$$

where $\epsilon_{\parallel}(\omega)$ indicates the $k \rightarrow 0$ limit of $\epsilon_{\parallel}(k, \omega)$. We see, that the latter expression involves the dielectric function in the long wavelength limit; a purely experimental quantity which can be measured with optical spectroscopy. At the same time this indicates some of the limitations: The large momentum sector is not accessible to optical spectroscopy. Measurement of this sector can be done using inelastic scattering of charged particles with large momentum transfer. At present the latter techniques do not yet meet the requirements of precision and stability necessary to detect the changes of spectral function associated with the onset of superconductivity, due to the fact that these changes are expected to be very tiny. Only if there is reason to suspect that the trends in temperature dependence of $\epsilon_{\parallel}(k, \omega)$ at large k are the same as for $\epsilon_{\parallel}(\omega)$, one may hope to extract some information about the correlation energy at somewhat higher momentum. It seems unlikely, though, that the contributions to the condensation energy near *e.g.* the (π, π) point could be estimated this way, and so far unexplored experimental techniques need to be developed which provide experimental access to the high momentum sector.

II. THE CORRELATION ENERGY IN THE SUPERCONDUCTING STATE

In the previous section we saw, that the Coulomb correlation energy within the j 'th layer

$$v_c^j = \frac{1}{(2\pi)^2} \int d^2\vec{k} V_k^j \langle \Psi_0 | \hat{\rho}_k^j \hat{\rho}_{-k}^j | \Psi_0 \rangle \quad (16)$$

can be calculated directly from knowledge of $\epsilon_k(\omega)$, which in principle can be determined experimentally using optical techniques or inelastic scattering of charged particles. Now we will make the connection to the pair-fluctuations induced by superconductivity.

In fact the fermions which become paired in the superconducting state in a conventional superconductor are the quasi-particles of the normal state Fermi-liquid. Note, that now we are using the Landau-Fermi-liquid concept of quasi-particles for the normal state. Later in this manuscript we will explore some consequences of *not* having a Fermi-liquid type normal state, where the quasi-particle concept will be abandoned. Although the quasi-particle eigenstates of a conventional Fermi-liquid have an amount of electron-character different from zero, their effective masses, velocities and scattering rates are renormalized. In terms of the quasiparticles the correlation energy is expressed as

$$v_c = \frac{1}{(2\pi)^3} \int d^3\vec{k} V_{\vec{k}}^{qp} g_{\vec{k}}^{qp} \quad (17)$$

where $V_{\vec{k}}^{qp}$ is the effective interaction between quasiparticles. The conventional point of view is, that pairing (enhancement of pair-correlations) reduces the correlation energy of the electrons, by virtue of the fact that in the superconducting state the paircorrelation function $g(r, r') = \langle \Psi | \hat{n}(r) \hat{n}(r') | \Psi \rangle$ increases at distances shorter than the superconducting coherence length ξ_0 . If the interaction energy $V^{qp}(r, r')$ is *attractive* for those distances, the correlation energy, Eq. 17, decreases in the superconducting state, and $V^{qp}(r, r')$ represents a (or the) pairing mechanism.

In the previous section we considered the Coulomb interaction, and we concluded that the correlation energy v_c arising from correlations follows directly from knowledge of $\epsilon_k(\omega)$. Before we continue the discussion we have to establish the connection between the expressions for the correlation energy involving the bare Coulomb interaction between electrons, and an effective interaction between the quasi-particle excitations of the normal state. In order to establish this connection, let us rewrite Eq. 9 for the Coulomb correlation energy in the form

$$v_c + v_0 = \frac{\hbar}{(2\pi)^4} \int d^3\vec{k} \int_0^\infty d\omega \text{Im} \frac{V_{\vec{k}}}{\epsilon(\vec{k}, \omega)} \tilde{\chi}_0(\vec{k}, \omega) \quad (18)$$

and the renormalized polarization $\tilde{\chi}_0(\vec{k}, \omega)$ is defined as $[1 - 1/\epsilon(\vec{k}, \omega)]/V_{\vec{k}}$. In the RPA it would correspond to

the bare polarization, but for a correlated system it represents all polarization diagrams, except those contained in the continued fraction of the RPA.

It is interesting, that in Eqs. 18 a *screened* interaction appears, multiplied with the renormalized polarization $\tilde{\chi}_0$. If the state of the system changes, the change of many-electron wavefunction results in a change $\tilde{\chi}_0 \rightarrow \tilde{\chi}_0 + \delta\tilde{\chi}_0$. Hence, the change of Coulomb correlation energy results *both* from a modification of the screened interaction $V_{\vec{k}}/\epsilon(\vec{k}, \omega)$ and of the polarization $\tilde{\chi}_0(\vec{k}, \omega)$.

From the decomposition in terms of $\tilde{\chi}_0(\vec{k}, \omega)$ we learn, that, unless the integration over ω is carried upto true ∞ , Eq. 18 will provide only the changes in interaction energy projected on a low energy scale. One should be careful not to limit the scale of integration too much, since changes in the low frequency sector of $\text{Im}\frac{-1}{\epsilon(\vec{k}, \omega)}$ can in principle be compensated by changes of opposite sign in the high energy sector. Theoretical guidance as to what is the relevant energy scales remains a crucial ingredient of any investigation of this type.

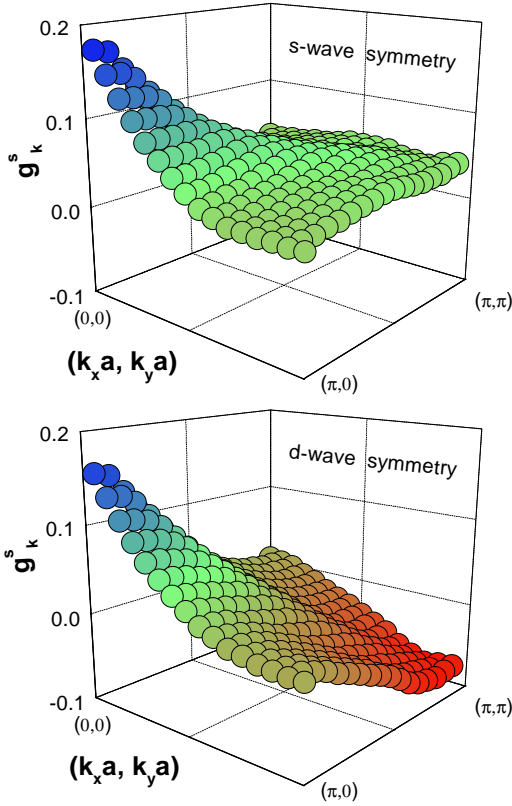


FIG. 1. The k -space representation of the superconductivity induced change of pair-correlation function for the s-wave (top panel) and d-wave symmetry (bottom panel). Parameters: $\Delta/W = 0.2$, $\omega_D/W = 0.2$. Doping level $x = 0.25$

Eq. 18 suggests that a simple connection can be made between the Coulomb correlation energy, and the inter-

action energy of the Landau-Fermi-liquid quasi-particles, Eq.17, which involves the *quasiparticle* paircorrelation function g_k^{qp} and the *effective* interaction V_k^{qp} between the quasiparticles. We should keep in mind, that the latter vertex may have a k - and ω -dependence which can be quite different from the Coulomb energy. Even simple RPA-screening of the Coulomb energy has a profound effect on the behaviour at small k . For example it replaces the diverging k^{-2} behaviour with a k -dependence which is well-behaved for small k .

For a Fermi liquid the paircorrelation function is

$$g_{n,k} = N_e^2 \delta_{k,0} + \sum_p f_p (1 - f_{p+k}) \quad (19)$$

The first term corresponds to the interaction between static density fluctuations in the solid. The second term represents the exchange correlations.

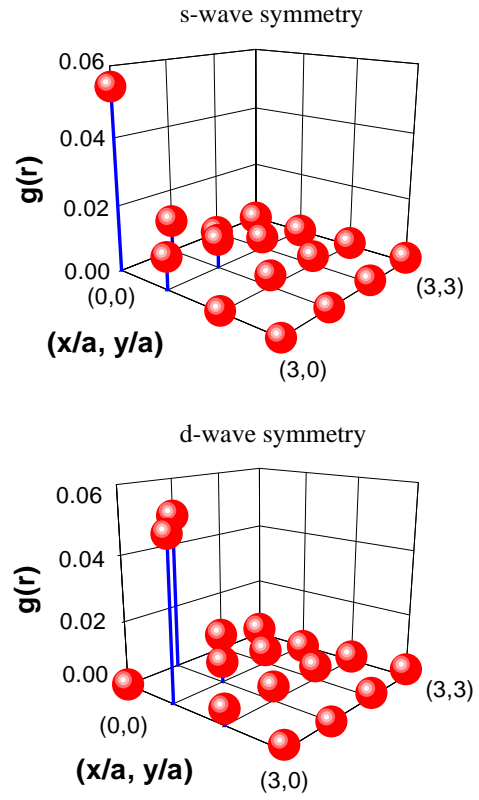


FIG. 2. The coordinate space representation of the superconductivity induced change of pair-correlation function for the s-wave (top panel) and d-wave symmetry (bottom panel). Parameters: $\Delta/W = 0.2$, $\omega_D/W = 0.2$. Doping level: $x = 0.25$

The projections of the operators $\hat{\rho}_k$ can be worked out for the BCS variational wavefunction, yielding $g_k^s = g_k - g_{n,k} = g_{X,k}^s + g_{\Delta,k}^s$, where $g_{X,k}^s$ is the change of the exchange correlation function induced by the super-

conducting state. Because it also exists in the normal state, it is usually assumed to be irrelevant to superconductivity. However, as we will see below, this term actually contributes significantly to the stabilization of d-wave superconductivity. The conventional 'anomalous' pair-correlation is $g_{\Delta,k}^s$.

$$\begin{aligned} g_{X,k}^s &= \sum_k (|u_{p+k}|^2 - \theta_{k+p}) (\theta_p - |u_p|^2) \\ g_{\Delta,k}^s &= \sum_p u_{p+k} v_{p+k} u_p^* v_p^* \end{aligned} \quad (20)$$

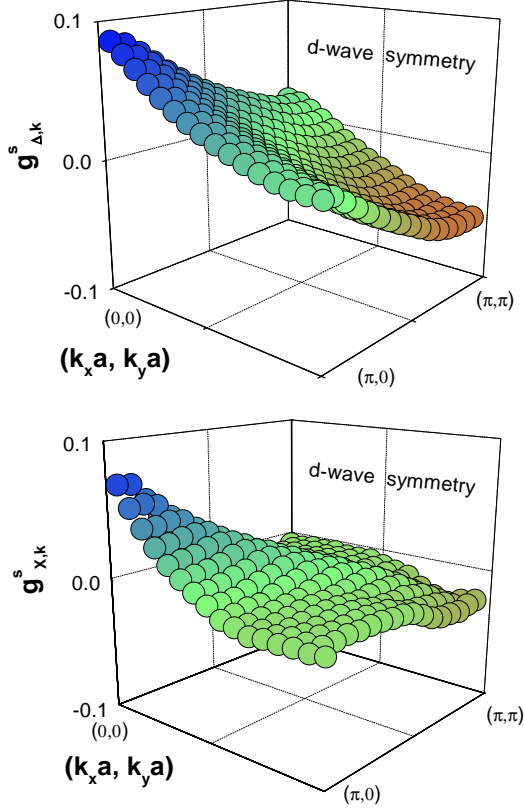


FIG. 3. The k-space representation of the 'anomalous' (top panel) and the exchange (bottom panel) superconducting contribution to the d-wave pair correlation function. Parameters: $\Delta/W = 0.2$, $\omega_D/W = 0.2$. Doping level $x = 0.25$

In Figs. 1,3, and 5 we show calculations of g_k^s , $g_{X,k}^s$ and $g_{\Delta,k}^s$ assuming a bandstructure of the form

$$\epsilon_k = \frac{W}{4} [\cos k_x a + \cos k_y a] - \mu \quad (21)$$

while adopting an order parameter of the form

$$\Delta_k = \Delta_0 \Theta(|\epsilon_k - \mu| - \omega_D) \quad (22)$$

for s-wave symmetry, and

$$\Delta_k = \Delta_0 [\cos k_x a - \cos k_y a] \Theta(|\epsilon_k - \mu| - \omega_D) \quad (23)$$

for d-wave symmetry. The parameters used were $\Delta/W = 0.2$, $\omega_D/W = 0.2$, and $E_F/W = 0.43$ corresponding to

$x=0.25$ hole doping counted from half filling of the band. The chemical potential in the superconducting state was calculated selfconsistently ($\mu/W = 0.39$ for d-wave, and $\mu/W = 0.40$ for s-wave symmetry) in order to keep the hole doping at the fixed value of $x=0.25$ [6].

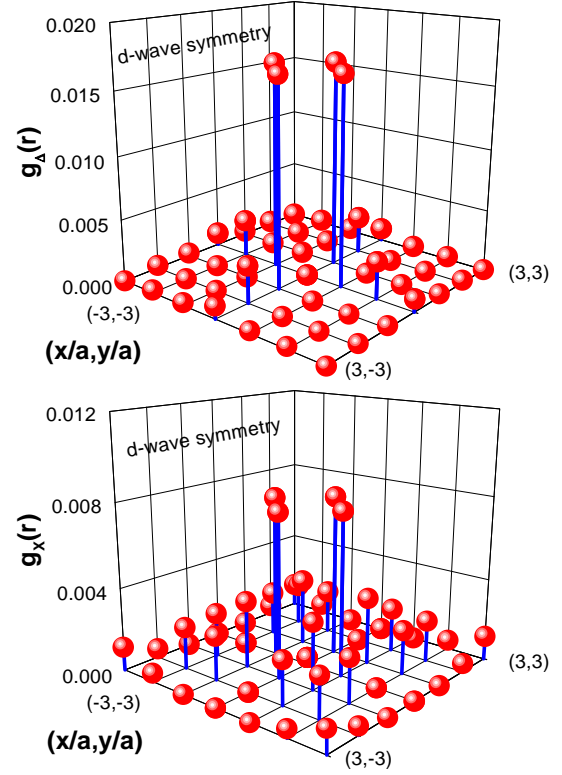


FIG. 4. The r-space representation of the 'anomalous' (top panel) and the exchange (bottom panel) superconducting contribution to the d-wave pair correlation function. Parameters: $\Delta/W = 0.2$, $\omega_D/W = 0.2$. Doping level $x = 0.25$

From Fig.1 we conclude that s-wave pairing symmetry requires a negative V_k regardless of the value of k , whereas the d-wave symmetry can be stabilized either assuming $V_k > 0$ for k in the (π, π) region, or $V_k > 0$ for k near the origin. Both types of symmetry are suppressed by a $V_k > 0$ at small momentum, such as the Coulomb interaction. Our numerical results show, that $g_{X,k}^s$ and $g_{\Delta,k}^s$ contribute about equally to the superconductivity related change of correlation function. The numerical results also show, that both for s-wave and d-wave symmetry $g_{X,k}^s$ is negative near the (π, π) point.

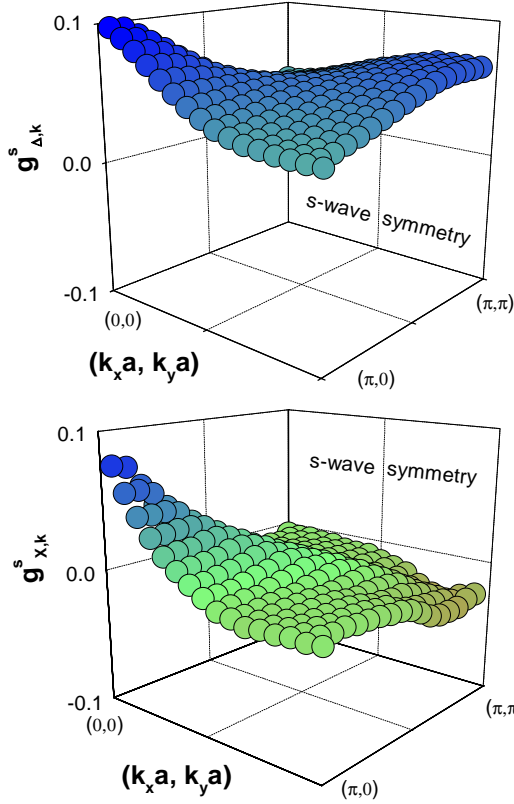


FIG. 5. The k -space representation of the 'anomalous' (top panel) and the exchange (bottom panel) superconducting contribution to the s -wave pair correlation function. Parameters: $\Delta/W = 0.2$, $\omega_D/W = 0.2$. Doping level $x = 0.25$

In Fig. 2 we display the correlation function in coordinate space representation ($g(r, r') = \sum_k \exp ik(r - r')g_k$). This graph demonstrates, that d -wave pairing is stabilized by a nearest-neighbor attractive interaction potential. An on-site *repulsion* has no influence on the pairing energy, since the pair-correlation function has zero amplitude for $r = 0$. On the other hand, for s -wave pairing the 'best' interaction is an on-site attractive potential, since the s -wave $g(r)$ reaches it's maximum value at $r = 0$.

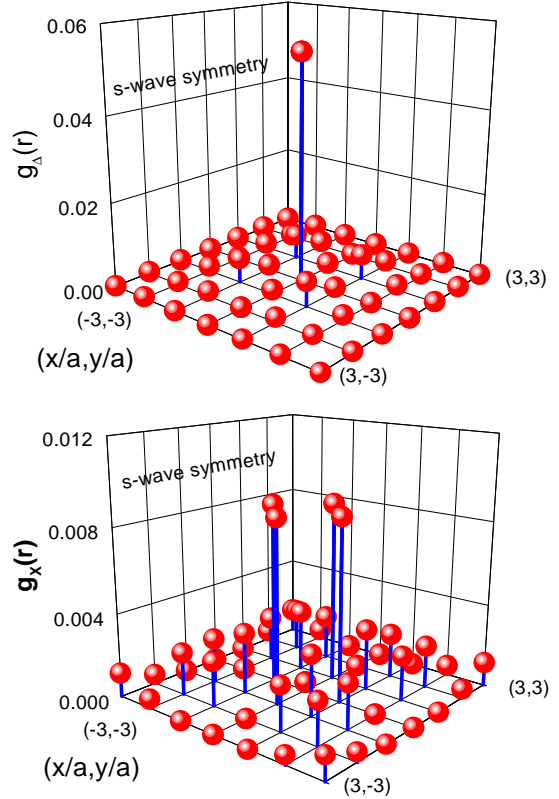


FIG. 6. The r -space representation of the 'anomalous' (top panel) and the exchange (bottom panel) superconducting contribution to the s -wave pair correlation function. Parameters: $\Delta/W = 0.2$, $\omega_D/W = 0.2$. Doping level $x = 0.25$

A. Experimental measurements of the Coulomb correlation energy

Experimentally the changes of Coulomb energy can be measured directly in the sector of k -space of vanishing k . The best, and most stable, experimental technique is to measure the dielectric function using spectroscopic ellipsometry, and to follow the changes as a function of temperature carefully as a function of temperature. Because the cuprates are strongly anisotropic materials, it is crucial to measure both the in-plane and out-of plane pseudo-dielectric functions, from which the full dielectric tensor elements along the optical axii of the crystal then have to be calculated. We followed this procedure for a number of different high T_c cuprates, using photons in the energy range 0.6 to 4 eV. Typical graphs of the Coulomb energy versus temperature are given in Fig. 7. In principle these curves should be summed over all frequencies, in order to provide the actual Coulomb energy stored in the small momentum k -sector.

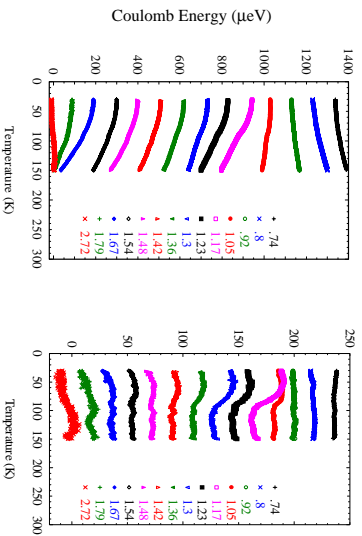


FIG. 7. Coulomb energy of optimally doped YBCO at $k=0$, $q=0$ as a function of temperature for various photon energies. The same values were assumed upto $k_{\parallel}=0.63\text{\AA}$, and integrated over k -space accordingly. The integration over $d\omega$ was carried out over 0.13 eV around each photon energy ω . All curves have been given arbitrary vertical offsets. In the right-hand panel a term proportional to T^2 has been subtracted from each curve.

Clearly the Coulomb energy in the superconducting state *increases* for $k=0$. This is completely expected, given the fact that the superconductivity induced change of the pair-correlation function $g_k > 0$ for $k \rightarrow 0$ (see Fig. 2). As also the Coulomb interaction is positive definite in this limit, the product $V_k g_k$ must increase in the superconducting state.

However, for $k \neq 0$ this need no longer be the case. Extrapolation of our data to finite k , either using Leggett's Eq. 4.1-5, or Eq. 15 which averages over all k_{\perp} , gives the results displayed in Fig. ???. We see, that the effect of including larger k_{\perp} compensates compensates to a large extent the increase in correlation energy at small k , and it even reverses the sign of the effect at higher photon energy. Yet clearly the overall effect is, that the Coulomb correlation energy increases in the superconducting state for small k . This implies, that the gain in free energy which is responsible for superconductivity must be sought either in other sectors of k -space (in particular at around the (π, π) point, see Fig. 1) or the kinetic energy itself is lowered in the superconducting state. The latter is only possible in a non-Fermi liquid scenario of the normal state.

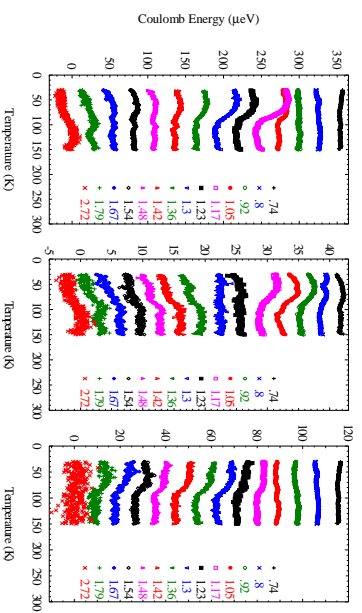


FIG. 8. Coulomb energy of optimally doped YBCO at $k=0$ as a function of temperature for various photon energies. The same values were assumed upto $k_{\parallel}=0.63\text{\AA}$, and integrated over k -space accordingly. The integration over $d\omega$ was carried out over 0.13 eV around each photon energy ω . Left panel: using the standard expression for $k=0$ and $q=0$. Middle panel: integrating over k_{\perp} using Eq. 15, Right panel: Using Leggett's Eq. 4.1-5 from Ref. [1]. All curves have been given arbitrary vertical offsets, and a T^2 background contribution has been subtracted from each curve.

III. THE KINETIC ENERGY

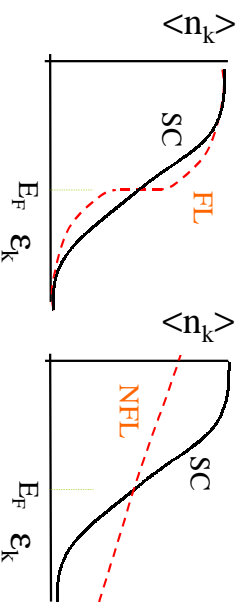


FIG. 9. Occupation function as a function of momentum in the normal (dash) and the superconducting (solid) state for Fermi-liquid (left panel) and a non-Fermi-liquid (right panel). The meaning of the horizontal axis is momentum labeled by the band parameter e_k .

In BCS theory an improvement of the correlation energy is partly compensated by a change of kinetic energy of opposite sign. This can be understood qualitatively in the following way: The correlated motion in pairs causes a localization of the relative coordinates of electrons, thereby increasing the relative momentum and the kinetic energy of the electrons. This is expressed quantitatively using the expression for the total kinetic energy of the electrons

$$E_{kin} = \sum_k n_k \epsilon_k \quad (24)$$

where $n_k = \sum_{\sigma} \langle \Psi | c_{k\sigma}^{\dagger} c_{k\sigma} | \Psi \rangle$ is the average occupation of states with momentum k . In the superconducting state

the Fermi-liquid step of n_k at the Fermi momentum is smoothed, as indicated in the left panel of Fig. 9, causing E_{kin} to become larger.

The ratio E_c/E_{kin} follows directly from the virial theorem. For example, if the only interaction present is the Coulomb interaction, $E_c/E_{kin} = -2$, and the same ratio applies to changes of these two energies induced by superconductivity. A pedagogical example where the kinetic energy of a pair is higher in the superconducting state, is provided by the negative U Hubbard model [7]: Without interactions, the kinetic energy is provided by the expression

$$E_{kin} = -t \sum_{\langle ij \rangle, \sigma} \langle \Psi | c_{i\sigma}^\dagger c_{j\sigma} | \Psi \rangle \quad (25)$$

Let us consider a 2D square lattice. If the band contains two electrons, the kinetic energy of each electron is $-2t$, the bottom of the band, hence $E_{kin} = -4t$. (In a tight-binding picture the reference energy is the center of the band irrespective of E_F , causing E_{kin} to be always negative). Let us now consider the kinetic energy of a pair in the extreme pairing limit, *i.e.* $U \gg t$, causing both electrons to occupy the same site, with a correlation energy $-U$. The occupation function n_k in this case becomes

$$n_k \approx \frac{1}{N_k} \frac{t}{U} \frac{1}{(1 + 4\epsilon_k/U)^2} \quad (26)$$

This implies that the kinetic energy approaches $E_{kin} \rightarrow -8t^2/U$. Hence the kinetic energy increases from $E_{kin}^n = -4t$ to $E_{kin}^s = -\frac{8t^2}{U}$ when the local pairs are formed.

The paired electrons behave like bosons of charge $2e$. A second order perturbation calculation yields an effective boson hopping parameter [8] $t' = t^2/U$. In experiments probing the charge dynamics, this hopping parameter determines the inertia of the charges in an accelerating field. As a result the plasma frequency of such a model would be

$$\omega_{p,s}^2 = 4\pi \frac{n}{2} (2e)^2 \frac{a^2 t^2}{\hbar^2 U} \quad (27)$$

whereas in the normal state

$$\omega_{p,n}^2 = 4\pi n e^2 \frac{a^2 t}{\hbar^2} \quad (28)$$

Because the plasma frequency is just the low frequency spectral weight associated with the conduction electrons, this demonstrates, that for conventional pairs (*i.e.* those which are formed due to correlation energy lowering) the expected trend is, that in the superconducting state the spectral weight *decreases*.

The same effect exists in the limit of weak pairing correlations. In [10] (Eq. 29, ignoring particle-hole asymmetric terms) the following expression was derived for the plasma resonance

$$\omega_{p,s}^2 = \frac{4\pi e^2}{V} \sum_k \frac{\Delta_k^2}{\hbar^2 E_k^3} \left[\frac{\partial \epsilon_k}{\partial k} \right]^2 \quad (29)$$

where V is the volume of the system. Integrating in parts, using that $\Delta_k^2 E_k^{-3} \partial_k \epsilon_k = \partial_k (\epsilon_k/E_k)$, and that $\partial_k \epsilon_k = 0$ at the zone-boundary, we obtain

$$\omega_{p,s}^2 = \frac{4\pi e^2}{V} \sum_k \frac{n_k}{m_k} \quad (30)$$

where $m_k^{-1} = \hbar^{-2} \partial^2 \epsilon_k / \partial k^2$. For a monotonous band dispersion the plasma frequency of the superconductor is always *smaller* than that of the unpaired system: Because the sign of the band-mass changes from positive near the bottom of the conduction band to negative near the top, the effect of the broadened occupation factors n_k is to give a slightly smaller average over m_k^{-1} , hence ω_p^2 is smaller. Note that the mass of free electrons does not depend on momentum, hence in free space ω_p^2 is unaffected by the pairing.

To obtain some feeling for the order of magnitude of the change of spectral weight, we consider a square band of width W with a Fermi energy $E_F = N_e/(2W)$, where N_e is the number of electrons per unit cell. To simplify matters we assume that $1/m_k$ varies linearly as a function of band energy: $1/m(\epsilon) = (W - 2E_F - 2\epsilon)/(Wm_0)$. We consider the limit where $\Delta \ll W, E_F$. Let us assume that the bandwidth ~ 1 eV, and $\Delta \sim 14$ meV corresponding to $T_c = 90$ K. The reduction of the spectral weight is then 0.28 %. If we assume that the bandwidth is 0.1 eV, the spectral weight reduction would typically be 11.4 %.

A. Kinetic energy driven superconductivity

If the state above T_c is *not* a Fermi liquid, the situation could be reversed. This situation is depicted in the righthand panel of Fig.9: A lowering of the total energy (or free energy at $T > 0$) could equally well be achieved from a kinetic energy lowering once pairs are formed, which then should be balanced by an increase of potential energy. This is not necessarily in contradiction with the virial theorem, even though at the end of the day all relevant interactions (including electron-phonon interactions) are derived from the Coulomb interaction: The superconducting correlations involve the low energy scale quasi-particle excitations and their interactions. These *effective* interactions usually have characteristics quite different from the original Coulomb interaction, resulting in $E_c/E_{kin} \neq -2$ for the low energy quasi-particles. Various models have been recently proposed involving pairing due to a gain of kinetic energy. In strongly anisotropic materials such as the cuprates, two possible types of kinetic energy should be distinguished: Perpendicular to the planes (along the *c*-direction) and along the planar directions.

B. Experimental determination of changes of the kinetic energy

A useful tool in the discussion of kinetic energy is the low frequency spectral weight (LFSW). LFSW is used to indicate the spectral weight associated with the conduction electrons. In infrared spectra this spectral weight is contained within a the 'Drude' conductivity peak centered at $\omega = 0$. Within the context of the tightbinding model a simple relation exists between the kinetic energy per site, with volume per site V_u , and the low frequency spectral weight [11]

$$E_{kin} = \frac{\hbar^2 V_u}{4\pi e^2 a^2} \omega_p^2 \quad (31)$$

Here the plasma frequency, ω_p , is used to quantify the LFSW:

$$\int_0^{\omega_m} \text{Re}\sigma(\omega) d\omega = \frac{1}{8} \omega_p^2 \quad (32)$$

where the integration should be carried out over the transitions within the valence tightbinding band. The upper limit ω_m serves as a reminder of that limitation.

C. The δ -function peak

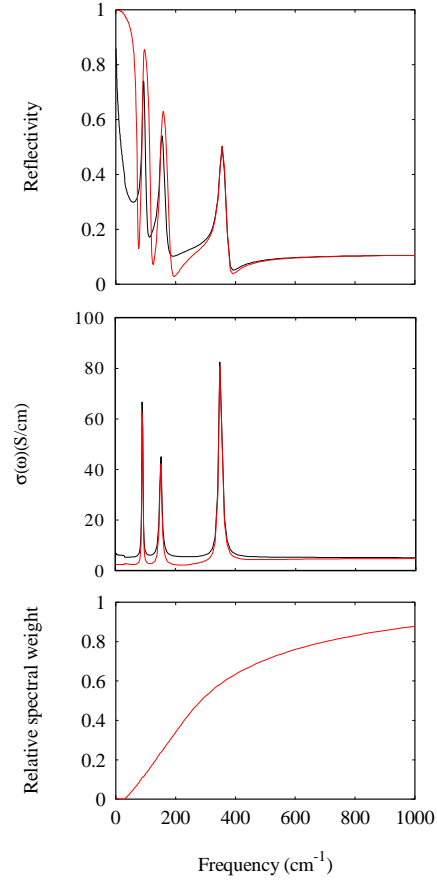


FIG. 10. reflectivity and conductivity in the normal (black) and s superconducting (red) state, and and spectral weight function using Kramers-Kronig analysis of the experimental spectra above 30 cm^{-1}

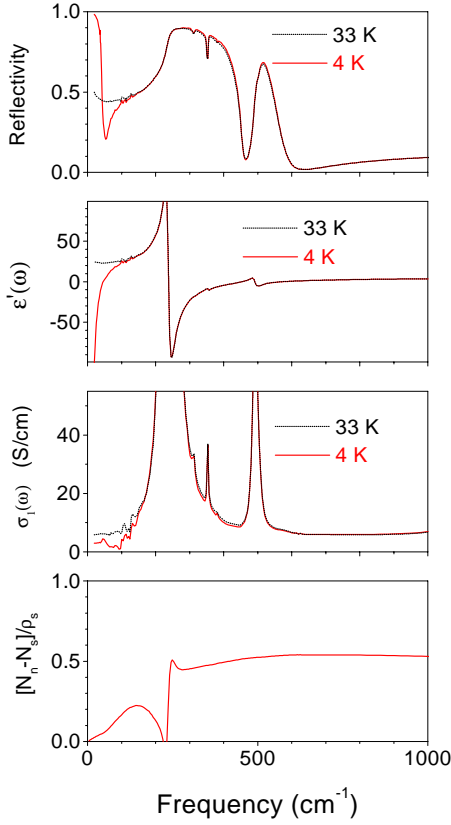


FIG. 11. C-axis optical spectra of optimally doped LSCO ($T_c=32$ K) [12]

The c-axis optical spectra of optimally doped high T_c cuprates look like the simulation of Fig. 10, which was generated from a dielectric function with model parameters for the normal state characteristic of c-axis transport in the cuprates: $1/\tau = 4000$ cm^{-1} , $\omega_p = 1000$ cm^{-1} . Due to the low conductivity along the c-direction of the cuprates, the c-axis conductivity is usually dominated by phonon contributions, below which the electronic spectrum can be barely distinguished.

The $\delta(\omega)$ peak in $\text{Re}\sigma(\omega)$ is of course not visible in the spectra directly. However the presence of the superfluid is manifested prominently in the London term of $\text{Re}\epsilon(\omega)$ (proportional to $\text{Im}\sigma(\omega)$): $\epsilon_L(\omega) = -\omega_{p,s}^2\omega^{-2}$. This is commonly used to determine the superfluid spectral weight, $\omega_{p,s}^2$, from the experimental spectra.

For the superconducting state a BSC s-wave gap was adopted, with $T_c = 100K$, and $2\Delta = 3.5k_B T_c$. In the lower panel the relative spectral weight function

$$\frac{8}{\omega_{p,s}(T)^2} \int_0^\omega \text{Re}[\sigma(\omega, 100K) - \sigma(\omega, T)] d\omega \quad (33)$$

is displayed. We see, that for frequencies of 4 times $2\Delta_{max}$ (220 cm^{-1}) about 90% of the spectral weight is

recovered.

According to the arguments given in section III A we conclude that $E_{kin,s} = E_{kin,n}$ if we observe, that all spectral weight originates from the far-infrared gap region, in agreement with the Glover-Tinkham-Ferrell sum rule, as is demonstrated in the lower panel of Fig. 10. If, on the other hand, superconductivity is caused by a gain of kinetic energy, part of $\omega_{p,s}^2$ originates from HESW. This implies, that $\omega_{p,s}^2$ is an upper limit to the kinetic energy change

$$E_{kin,s} - E_{kin,n} < -\frac{\hbar^2 V_u}{4\pi e^2 a^2} \omega_{p,s}^2 \quad (34)$$

On the other hand, a more precise determination of $E_{kin,s} - E_{kin,n}$ is obtained by measuring experimentally the amount of HESW transferred to the $\delta(\omega)$ peak due to the passage from the normal to the superconducting state. If for example the experiments would look like Fig.10, we would conclude that less than 10% of the $\delta(\omega)$ peak is associated with the kinetic energy gain.

A characteristic example of this behaviour is observed in LSCO, Fig. 11. In $\epsilon'(\omega)$ of LSCO the superfluid response shows up very clearly as a zero-crossing, corresponding to the c-axis plasma edge [15,12] at around 50 cm^{-1} .

The oscillator strength of the $\delta(\omega)$ peak was obtained from the low frequency limiting behaviour of the real part of the dielectric function (not displayed): $\omega^2 \epsilon'(\omega) \rightarrow \omega_{p,s}^2$. These data appear to suggest, that in this case the GTF rule is not satisfied, and about 50 % of the spectral weight originates from high energies. Observations similar to this have been reported in a series of papers by *et al.* [28]. However, experimental artifacts caused by a very small amount of mixing of ab-plane reflectivity into the c-axis reflectivity curves may have resulted in an overestimation of the spectral weight originating from high energies. In Appendix B we demonstrate, that small systematic errors in the measured reflectivities due to polarization leakage, strongly affect the spectral weight functions resulting from the Kramers-Kronig analysis. The conditions like those used for Fig. 11 typically correspond to 1 percent leakage of ab-plane reflectivity into the signal. In the appendix we show that this causes an artificial 30 % deviation from the GTF rule, similar to the behaviour seen in the lower panel of Fig. 11.

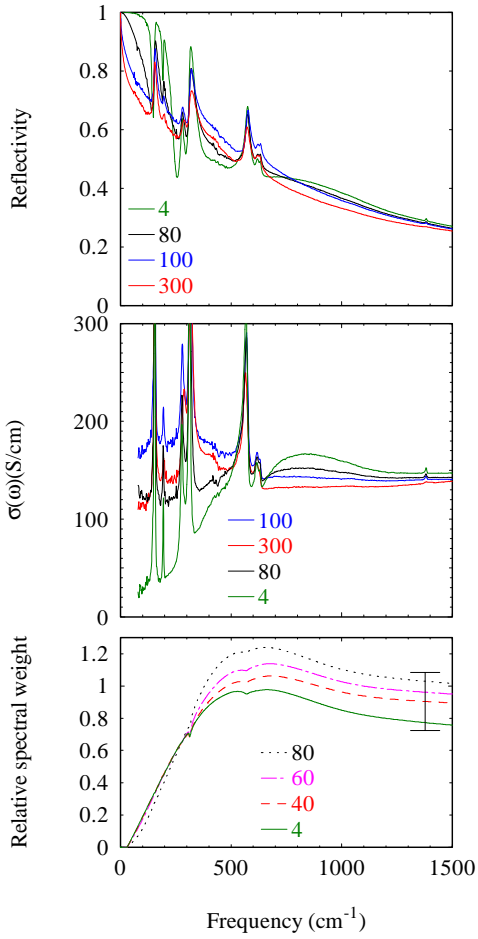


FIG. 12. C-axis optical spectra of optimally doped YBCO ($T_c=92$ K) [17]

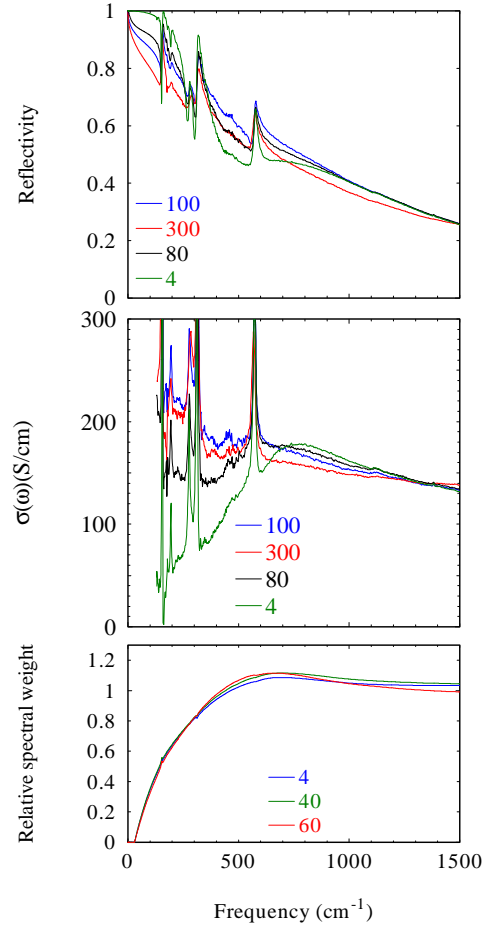


FIG. 13. C-axis optical spectra of overdoped YBCO ($T_c=92$ K) [17]

The effect of polarization leakage is particularly large in LSCO, and in other highly anisotropic HTSC, because the electronic $\sigma_c(\omega)$ is usually very low due to the 2-dimensionality. One of the highest $\sigma_c(\omega)$'s is observed in optimally doped and overdoped YBCO. The larger $\sigma_c(\omega)$ causes the c-axis reflectivity to be much larger at all frequencies, thereby minimizing the effect of leakage of R_{ab} into the c-axis reflectivity spectra on the data-analysis. C-axis reflectivity data [17] of optimally doped and overdoped YBCO are shown in Figs.12 and 13. Above T_c the optical conductivity is weakly frequency dependent, and does not resemble a Drude peak. Below T_c the conductivity is depleted for frequencies below 500 cm^{-1} , reminiscent of the opening of a large gap, but not an s-wave gap, since a relatively large conductivity remains in this range.

The c-axis optical conductivity is one order of magnitude larger than for LSCO near optimal doping. As a result the relative importance of the optical phonons in the spectra is diminished. In the case of YBCO, the experiments indicate no significant transfer of spectral weight from high frequencies associated with the onset

of superconductivity. In fact, there is a slight overshoot in the region between 500 and 700 cm^{-1} , due to the fact that the normal state and superconducting state curves cross at 600 cm^{-1} . In the case of YBCO this could be explained as a result of the presence of several superconducting layers per unit cell, resulting in a 'second plasma' mode. In essence this is an out-of-phase oscillation of the two individual components. This mode has been predicted in Ref. [18] for the case of a multilayer of Josephson coupled 2D superconducting layers. The existence of two longitudinal modes was confirmed experimentally in $\text{SmLa}_{0.8}\text{Sr}_{0.2}\text{CuO}_{4-\delta}$ [19].

For the sum-rule the presence of this extra mode makes no difference. The extra spectral weight in the superconducting state associated with this mode has in principle the same origin as the spectral weight in the zero-frequency δ -function. In a conventional picture the source would be the spectral weight removed due to a depletion of $\sigma_c(\omega)$ in the gap-region. The implementation of the sum-rule relevant for this case then states that the relative spectral weight function, Eq. 33, overshoots the 100 % line close to the 'second plasma' mode, and saturates at 100 % for frequencies far above this mode. This is indeed observed in Figs. 12 and 13.

D. Kinetic energy perpendicular to the planes

C-axis kinetic energy driven superconductivity has been proposed within the context of interlayer tunneling, and has been extensively discussed in a number of papers [20–30]. One of the main reasons to suspect that superconductivity was c-axis kinetic driven, was the observation of "incoherent" c-axis transport of quasiparticles in the normal state [31] and, rather surprisingly, *also* in the superconducting state [12,14,13], thus providing a channel for kinetic energy lowering for charge carriers as soon as pairing sets in. Because the Josephson coupling energy corresponds to the interlayer *pair*-hopping amplitude, it corresponds to the upper limit of the change of kinetic energy between the normal and superconducting state [21,22]. It only provides an upper limit, because the Josephson coupling energy is, apart from universal prefactors, the amount of spectral weight of the $\delta(\omega)$ conductivity-peak. The high energy spectral weight transferred to the $\delta(\omega)$ -peak can not exceed this amount. This allowed a simple experimental way to test the idea of c-axis kinetic energy driven superconductivity by comparing the experimentally measured values of the condensation energy (E_{cond}) and E_J . The ILT hypothesis requires that $E_J \approx E_{cond}$. In the spring of 1996 the first experimental results were presented [24] for Tl2201 ($T_c=80$ K), showing that E_J was at least two orders of magnitude too small to account for the condensation energy, confirmed later by more precise measurements of λ_c [27] of 17 μm and the Josephson plasma resonance

(JPR) [26] at 28 cm^{-1} , allowing a precise determination of $E_J \approx 0.3\mu\text{eV}$ in Tl2201 with $T_c = 80$ K. This is a factor 400 lower than $E_{cond} \approx 100\mu\text{eV}$ per copper, based either on c_V experimental data [33], or on the formula $E_{cond} = 0.5N(0)\Delta^2$ with $N(0) = 1\text{eV}^{-1}$ per copper, and $\Delta \simeq 15\text{meV}$. In Fig. 14 the change in c-axis kinetic energy and the Josephson coupling energies are compared to the condensation energy for a large number of high T_c cuprates. For most materials we see, that $E_J < E_{cond}$, sometimes differing by several orders of magnitude.

However, as stressed above, E_J provides only an *upper limit* for ΔE_{kin} . A c-axis kinetic energy change *smaller* than E_J is obtained if we take into account the fact that a substantial part of $\delta(\omega)$ -function is just the spectral weight removed from the sub-gap region of the optical conductivity. Usually it is believed that in fact this is the *only* source of intensity of spectral weight for the δ -function, known as the (phenomenological) Glover-Tinkham-Ferrell [34] sum-rule. Recent data of Basov *et al.* indicated that for underdoped materials about 60% comes from the subgap region in the far infrared, while about 40% originates from frequencies much higher than the gap, whereas for optimally doped cuprates at least 90% originates from the gap-region, while less than 10% comes from higher energy. In Appendix A we show, that systematic errors in Ref. [28] have probably resulted in a substantial overestimate of the amount of HESW transferred to the δ -function. In summary $\Delta E_{kin,c} < 0.1E_J$ in most cases, implying that the discrepancy between E_{cond} and ΔE_{kin} is even a factor 10 larger than implied by Fig.14.

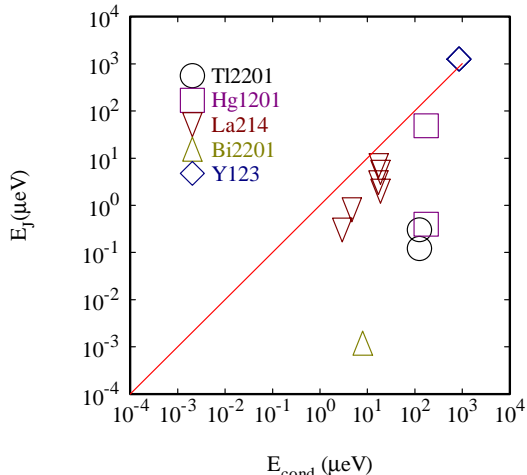


FIG. 14. Intrinsic Josephson coupling energy [12,27,26,28–30,35,25,17] versus condensation energy [33].

E. Kinetic energy parallel to the planes

In-plane kinetic energy driven superconductivity has been proposed by a number of researchers: Hirsch [20,36] discussed this possibility as a consequence of particle-hole asymmetry. It has also been discussed within the context of holes moving in an anti-ferromagnetic background [37]. More recently the possibility of a kinetic energy gain associated with pair-hopping between stripes has been suggested [38], and an in-plane pair-delocalization mechanism have been proposed by Anderson [39].

A major issue is the question how to measure this. The logical approach would be, to measure again $\sigma(\omega, T)$ using the combination of reflectivity and Kramers-Kronig analyses, and then compare the spectral weight function in the superconducting state to the same above T_c . There are several weak points to this type of analyses. In the first place there is the problem of sensitivity and progression of experimental errors: Let us assume, that the change of kinetic energy is of order 0.1 meV per Cu atom

(this is approximately the condensation energy of the optimally doped single layer cuprate Tl2201, with $T_c = 85$ K.). For an interlayer spacing of 1.2 nm, this corresponds to a spectral weight change $\Delta(\nu_p^2) = 10^5 \text{ cm}^{-2}$. As the total spectral weight in the far infrared range is of order $\nu_p^2 = 14000^2 \text{ cm}^{-2}$, the relative change in spectral weight is of order 0.05 %. Typical accuracy reached for spectral weight estimates using conventional reflection techniques is of order 5%. This illustrates the technical difficulties one has to face when attempting to extract superconductivity induced changes of the kinetic energy and Coulomb energy.

Experimental limitations on the accuracy are imposed by (i) the impossibility to measure *all* frequencies including the sub-mm range, (ii) Systematic errors induced by Kramers-Kronig analysis: The usual procedure is to use data into the VIS/VUV regime and beyond for completing the KKA in the far infrared, assuming that no important temperature dependence is present outside the far infrared range. Obviously this assumption becomes highly suspicious if the search is concentrated on spectral weight transfer originating from precisely this frequency range.

The remedy is, to let nature perform the spectral weight integral. Due to causality $\text{Re}\epsilon(\omega)$ and $\text{Re}\sigma(\omega)$ satisfy the Kramers-Kronig relation

$$\text{Re}\epsilon(\omega) = 1 - \int_0^\infty \frac{8\sigma(x)}{\omega^2 - x^2} dx \quad (35)$$

The main idea of SWT is, that spectral weight is essentially transferred from the interband transitions at an energy of several eV, down to the δ -function in $\sigma(\omega)$ at $\omega = 0$. If this is the case, we have $x = 0$ for the extra spectral weight in relation 35. Together with Eq. 34 it follows, that changes in kinetic energy can be read directly from $\text{Re}\epsilon(\omega)$ using the relation

$$\delta E_{kin}^{eff}(\omega) = \frac{4\hbar^2 \omega^2 V_u}{\pi e^2 a^2} \text{Re}\delta\epsilon(\omega) \quad (36)$$

If the spectral weight is transferred to a frequency range ω_0 , than the above expression can still be applied for $\omega \gg \omega_0$. If we measure $\text{Re}\epsilon(\omega)$ *directly* using spectroscopic ellipsometry, then indeed nature does the integration of $\sigma(\omega)$ for us at each temperature. This eliminates to a large extent various systematic and not so systematic errors affecting the overall accuracy of the SW-sum. It is important, to measure $\delta E_{kin}^{eff}(\omega)$ at a number of different frequencies, and check whether a convergent result is obtained. If so, this proves experimentally that there is SWT to frequencies well below the range of ω used in the experiment. In order to separate redistribution of spectral weight within the quasi-Drude infrared peak from high energy SWT processes, the best optical range for measuring $\delta E_{kin}^{eff}(\omega)$ is between 0.5 and 1 eV. This is above the frequencies where the main spectral weight

of the quasi-Drude peak is located, while it is below the main interband transitions.

The second problem is, that already above the superconducting phase transition the optical spectra of these materials have appreciable temperature dependence. What we really like to measure is the spectra of the same material in the superconducting state, and in the 'normal' state, both at the same temperature. Typical magnetic fields required to bring the material in the normal state are impracticable, let alone the complications of magneto-optics which then have to be faced. A more practical approach is to measure carefully the temperature dependence over a large temperature range, with small temperature intercepts, and to search for changes which occur at the phase transition.

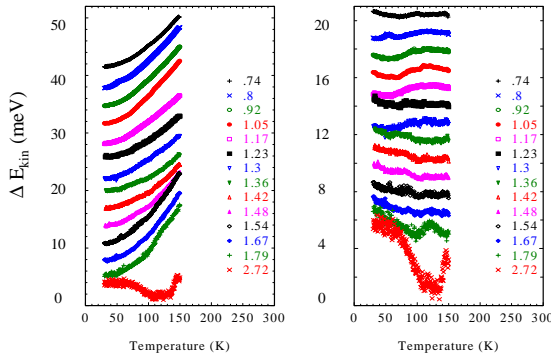


FIG. 15. Measured values of $E_{kin}^{eff}(\omega, T)$ of optimally doped YBCO ($T_c=92$ K). All curves have been given arbitrary vertical offsets. In the righthand panel a T^2 background contribution has been subtracted from each curve. Only the universal (photon energy independent for $\hbar\omega \rightarrow 0$) trends and amplitudes in the temperature dependence can be attributed to the temperature dependence of the kinetic energy.

In Fig. 15 the function $E_{kin}^{eff}(\omega, T)$ is shown as a function of temperature for a number of different photon energies for the case of $\text{YBa}_2\text{Cu}_3\text{O}_7$. We observe, that in the superconducting state the kinetic energy drops by an amount of about 1 meV per Cu. This is in fact a relatively large effect. This surprising result seems to tell us, that in the cuprates the kinetic energy in the superconducting state is *lowered* relative to the normal state. This corresponds to the unconventional scenario depicted in the righthand panel of Fig.9, where the normal state is a non-Fermi liquid, whereas the superconducting state follows the behaviour of a (more) conventional BCS-type wavefunction with ditto quasiparticles. The amazing conclusion from this would be, that there is no need to for a *lowering* of the correlation energy any more.

However, we also notice from the same figure, (i) that

$\Delta E_{kin}^{eff}(\omega, T)$ looks smaller at the lowest photon energies, and (ii) that $\Delta E_{kin}^{eff}(\omega, T)$ changes sign at around $\hbar\omega = 1.2$ eV. This suggests, that these changes of ϵ' are actually a signature of a relative narrow resonance centered at 1.2 eV. Similar temperature dependent changes have been reported by Holcomb *et al.* [32], based on differential reflection spectroscopy. We have checked, that our temperature dependence of the real and imaginary part of $\epsilon(\omega)$ agree quantitatively with the temperature dependent reflection coefficients reported by these authors. In Fig. 16 we analyzed the superconductivity induced changes of $\epsilon'(\omega)$ and $\epsilon''(\omega)$ simultaneously using the following model for the superconductivity induced change of dielectric function:

$$\delta\epsilon(\omega) = \epsilon_s(\omega) - \epsilon_n(\omega) = \frac{\omega_{p,0}^2}{\omega(\omega + i\gamma) - \omega_0^2} + \frac{\pi e^2 a^2}{4V_u} \frac{\delta E_{kin}^{eff}}{\hbar^2 \omega^2} \quad (37)$$

Little *et al.* [32] have attributed such superconductivity induced depletion of spectral weight at around 1.2 eV to the coupling of the conduction electrons to narrow band of excitations in this range, which in turn in a strong coupling formalism could be the mechanism causing superconductivity. The situation where $4\hbar^2\omega_{p,0}^2V_u/(\pi e^2 a^2) = \delta E_{kin}^{eff}$ corresponds to full transfer of the spectral weight lost at the frequency $\omega_0 = 1.2$ eV to the zero frequency δ -peak. Whether or not such transfer of spectral weight is implied by the strong coupling to a 1.2 eV mode still needs to be clarified in the near future. The condensation energy of optimally doped YBCO is about 4 J/g.at ([33]), which corresponds to 0.5 meV per unit cell, or 0.17 meV per Cu atom. In the figure we also indicate attempts to fit this with $\delta E_{kin}^{eff} = 0.5$ meV (the conventional BCS prediction, see Eq.30), and $\delta E_{kin}^{eff} = -0.5$ meV, the value needed if superconductivity is caused by a lowering of kinetic energy. However, we should keep in mind that this is only an effective number, which is only exactly the kinetic energy if the bands follow the simplest single orbital tightbinding behaviour. The actual number for the kinetic energy may come out quite differently depending on the model used for the band dispersion.

The best fits were obtained for -0.2 meV $< \delta E_{kin}^{eff} < 0.03$ meV, indicating a possible gain of kinetic energy in the superconducting state of order 0.1 meV per unit cell (3 copper atoms).

YBCO thin film
change in dielectric function
 $\epsilon_s - \epsilon_n$

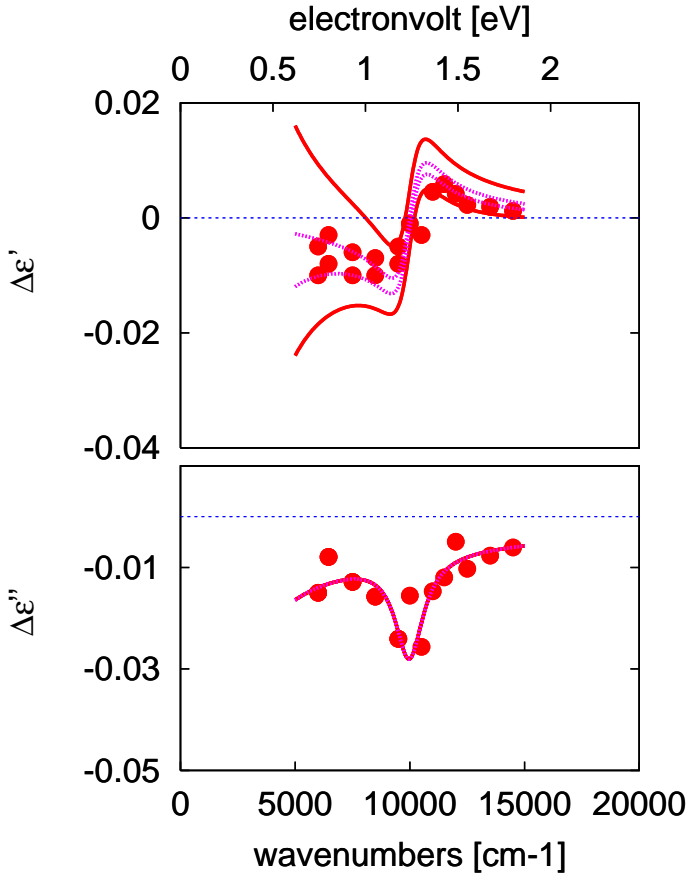


FIG. 16. Superconductivity induced change of $\epsilon'(\omega)$ and $\epsilon''(\omega)$ as a function of frequency, measured at $T=60$ K. The fits correspond to Eq. 37 with parameters: $\omega_{p,0}/2\pi c = 550$ cm^{-1} , $\omega_0/2\pi c = 10000$ cm^{-1} , $\gamma/2\pi c = 1500$ cm^{-1} , and $\delta E_{kin}^{eff} =$ (from top to bottom) 0.5 meV, 0.03 meV, -0.2 meV, -0.5 meV.

IV. CONCLUSIONS

We discussed optical techniques to measure changes in kinetic energy and Coulomb energy associated with the superconducting state. We demonstrated, that the correlation functions are qualitatively different for s- and d-wave pairing, demonstrating rather directly that quite different s- and d-wave pairing are stabilized by a different mechanism. We provided experimental evidence, that in YBCO the correlation energy *increases* in the long wavelength limit when the system enters the superconducting state. We showed, that the kinetic energy change along the c-direction is orders of magnitude lower than the condensation energy. We introduce an experimental technique based on ellipsometric spectroscopy to measure the changes of in-plane kinetic energy. We show for optimally doped YBCO, that the change of in-plane

kinetic energy due to superconductivity is in the interval $-0.2\text{meV} < \delta E_{kin} < 0.03\text{meV}$ per unit cell.

V. ACKNOWLEDGEMENTS

These notes cover experiments by postdocs and Ph D students working in my lab, part of which have been reproduced in these lecture notes, and who deserve full credit for their invaluable time and energy devoted to careful experiments, in particular, and addition to those indicated in the header of this manuscript, G. Rietveld, J.H. Kim, J. Schuetzmann, A. Tsvetkov, B. J. Feenstra, H. S. Somal, and D. Dulic. We are greatly indebted to A. A. Menovsky, S. Uchida, A. Erb, N. Kolesnikov, Z.F. Ren, W. N. Hardy, and B. Willemsen and their collaborators, for producing and generously supplying single crystals and thin films, optical data of which have been partly reproduced from earlier publications in these notes. The development of the theoretical concepts discussed in these lecture notes, has been greatly enhanced by numerous discussions with, and generous sharing of ideas by D. I. Khomskii, G. A. Sawatzky, M. J. Rice, P. W. Anderson, A. J. Leggett, Z.X. Shen, S.C. Zhang, S. Chakravarty, M. Turlakov, J.E. Hirsch, D. Basov, A. J. Little, and M. Norman.

VI. APPENDIX: SYSTEMATIC ERRORS IN DETERMINING ΔE_{KIN} FROM REFLECTION SPECTRA

Recently infrared results have been published on Tl2201 providing values of the c-axis penetration depth [28]. In addition an analysis of the temperature dependence of the spectral weight was given, indicating an unconventional evolution of the interlayer conductivity through T_c . This was used to argue, that the effective mass in the superconducting state is reduced as compared to the normal state. The data were obtained on a mosaic of several crystals of thickness 80 μm . Here we demonstrate that systematic errors in the polarization of the light, are strongly amplified in the spectral weight analysis, and can in fact cause an apparent superconductivity induced transfer of high energy spectral weight to the far infrared region of the magnitude and sign reported in Refs. [28].

To illustrate this, we use the "synthetic data" described in section III C. Important for the present discussion is that this conductivity satisfies the Glover Ferrell Tinkham sumrule. To check the reliability of the Kramers-Kronig relations for the experimental data, the synthetic dielectric functions were used to generate synthetic reflectivity spectra in the range from 30 to 9000 cm^{-1} . These were extrapolated and Kramers-Kronig analyzed

using the same routines as those used for the experimental data. The resulting conductivities and the spectral weight function showed no significant deviations as a result of the data analysis, as compared to the original conductivities used on input of the Kramers-Kronig analysis. Let us now check the robustness vis a vis experimental errors in the reflectivity spectrum. An often occurring error with small samples, particularly hazardous if they are strongly anisotropic, is leakage of the unwanted polarization (a-axis in this case) in the reflection spectrum of the wanted polarization (c-axis in this case). The source of this can be manifold:

- crystal imperfections
- diffraction of the reflected signal at boundaries of the individual crystals forming the mosaic
- imperfect functioning of the polarizer
- imperfect alignment of some of the crystals forming the mosaic
- imperfect alignment of the polarizer

In the case of a-axis reflectivity leaking into the c-axis spectrum, the net effect is to replace R_c with $(1-x)R_c + xR_{ab}$, where R_{ab} and R_c are the in-plane and c-axis reflectivity respectively and x is the amount of leakage. Because in the far infrared R_{ab} is close to 100 percent, a small leakage can have considerable effect. In Fig. 17 a leakage of only 1 percent was assumed. Although the Kramers-Kronig analysis still produces inconspicuously looking optical conductivities, the spectral weight analysis is severely flawed: The saturation level sinks from 100 percent to about 70 percent. This is the result of a polarization leakage of 1%.

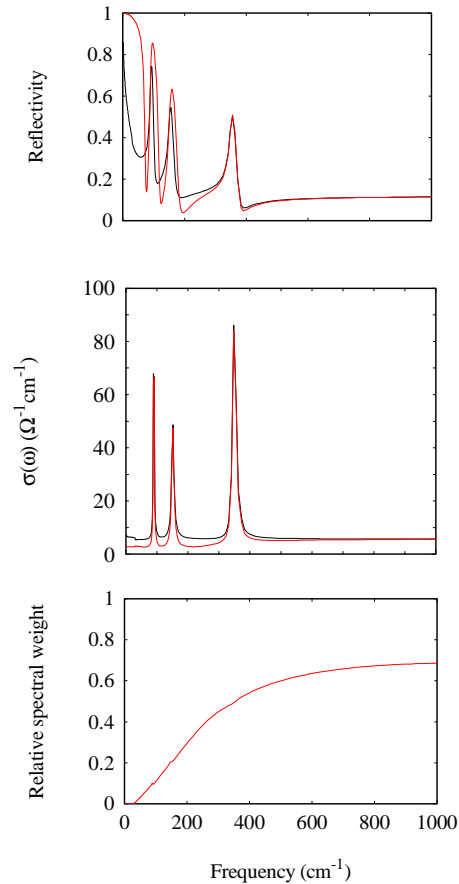


FIG. 17. Same analysis as in Fig.10, except that the reflection data have been replaced with $0.99R_c + 0.01R_{ab}(\omega)$.

The systematic errors in reflectivity spectra can be particularly large when working with mosaics of several crystals, rather than a large single crystal. The result can even be a crossing of the conductivity curves as indicated in Fig. 18, making the transfer of spectral weight appear to be negative, while in fact the sample properties are those displayed in fig.10

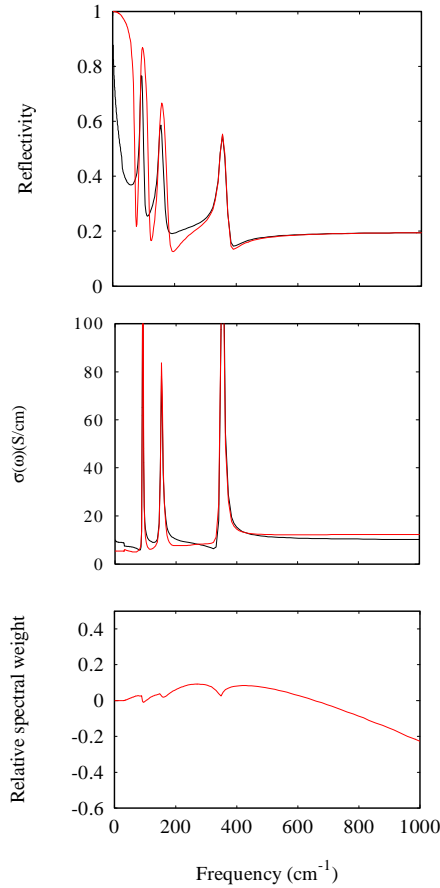


FIG. 18. Same analysis as in Fig.10, except that the reflection data have been replaced with $0.9R_c + 0.1R_{ab}$.

Especially for small samples, and for samples with a small value of the c-axis conductivity, the amplification of this kind of errors is rather dramatic.

[1] A. J. Leggett, Proc. Natl. Acad. Sci. USA Vol. **96** (1999) 8365-8372
 [2] P. Nozieres, and D. Pines, Phys. Rev. **111** (1958) 442; *ibid.* **113** (1959) 1254-1267.
 [3] Note the extra factor of π . In Ref. [2] this factor is absent, but it is recuperated in the final formulas.
 [4] A. L. Fetter, Annals of Physics **88** (1974) 1-25
 [5] DvdM is indebted to Misha Turlakov for correcting the expressions presented in this subsection.
 [6] D. van der Marel, Physica C **165** (1990) 35-43; D. van der Marel, and G. Rietveld, Phys. Rev. Lett. **69** (1992) 2575-2577; G. Rietveld, N. Y. Chen, D. van der Marel, Phys. Rev. Lett. **69** (1992) 2578-2581; D. van der Marel, D. I. Khomskii and G.M. Eliashberg, Phys. Rev. B **50** (1994) 16594-16597.

[7] R. Micnas, J. Ranninger, and S. Robaszkiewicz, Rev. Mod. Phys. **62**, 113 (1990).
 [8] P. Nozieres, and S. Schmitt-Rink, J. Low Temp. Phys **59** (1985) 195.
 [9] M. R. Norman, M. Randeria, B. Janko, J. C. Campuzano, Phys. Rev. B **61** 14724 (2000).
 [10] D. van der Marel, Phys. Rev. B. **51** (1995) 1147.
 [11] P. F. Maldague. Phys. Rev. B **16** (1977) 2437.
 [12] Jae H. Kim, H.S. Somal, D. van der Marel, A.M. Gerrits, A. Wittlin, V.H.M. Duijn, N.T. Hien and A.A. Menovsky, Physica C **247** (1995) 297-308.
 [13] A. Hosseini *et al.*, Phys. Rev. Lett. **81** (1998) 1298.
 [14] D. Dulic, D. van der Marel, A. A. Tsvetkov, W. N. Hardy, Z. F. Ren, J. H. Wang, B. A. Willemsen, Phys. Rev. B, **60** (1999) R15051.
 [15] K. Tamasaku, Y. Nakamura, and S. Uchida, Phys. Rev. Lett. **69** (1992) 1455.
 [16] D. Basov *et al.*, Science **283** (1999) 49
 [17] M. Grueninger, D. van der Marel, A.A. Tsvetkov, A. Erb, Phys. Rev. Lett. **84** (2000) 1575.
 [18] D. van der Marel and A. Tsvetkov, cond-mat/9609155; *ibid.*, Czechoslovak Journal of Physics 46, Part S6 (1996) 3165.
 [19] H. Shibata, T. Yamada, Phys. Rev. Lett. **81**, 3519 (1998).
 [20] J. E. Hirsch, Physica C **201** (1992) 347.
 [21] P. W. Anderson, Science **268** (1995) 1154.
 [22] A. J. Leggett, Science **274** (1996) 587.
 [23] S. Chakravarty, Eur. Phys. J. B **5** (1998) 337.
 [24] D. van der Marel, H.S. Somal, B.J. Feenstra, J.E. van der Eb, J. Schuetzmann, Jae Hoon Kim. Proc. 10th Ann. HTS Workshop on Physics, Houston, World Sc. Publ. (1996) 357-370; J. Schuetzmann, H.S. Somal, A.A. Tsvetkov, D. van der Marel, G. Koops, N. Koleshnikov, Z.F. Ren, J.H. Wang, E. Brueck and A.A. Menovski. Phys. Rev. B **55** (1997) 11118.
 [25] C. Panagopoulos *et al.*, Phys. Rev. Lett. **79** (1997) 2320
 [26] A. Tsvetkov *et al.*, Nature **395** (1998) 360.
 [27] K. A. Moler *et al.*, Science **279** (1998) 1193.
 [28] D. Basov *et al.*, Science **283** (1999) 49.
 [29] J. Kirtley *et al.*, Phys. Rev. Lett. **81** (1998) 2140
 [30] M.B. Gaifullin *et al.*, Phys. Rev. Lett. **83** (1999) 3928
 [31] S. L. Cooper, and K.E. Gray, *Physical properties of High Temperature Superconductors IV*, ed. D. M. Ginsberg (World Scientific, Singapore 1994).
 [32] M. J. Holcomb *et al.* Phys. Rev B **53** (1996) 6734; W. A. Little *et al.*, J. Superconductivity **12** (1999) 89-94;
 [33] J. W. Loram, K. A. Mirza, J. M. Wade, J. R. Cooper, and W. Y. Liang, Physica C **235-240** (1994) 134.
 [34] M. Tinkham, and R. A. Ferrell, Phys. Rev. Lett. **2** (1959) 331.
 [35] T. Shibauchi *et al.*, Phys. Rev. Lett. **72** (1994) 2263
 [36] J. E. Hirsch, and F. Marsiglio, Physica C **331** (1999), 150-156.
 [37] J. Bonca, P. Prelovsek, and I. Sega, Phys. Rev. B **39** (1989) 7074; J. A. Riera, Phys. Rev. B **40** (1989) 833; Y. Hasegawa, and D. Poilblanc, Phys. Rev. B **40** (1989) 9035; E. Dagotto, J. Riera, and A.P. Young, Phys. Rev. B **42** (1990) 2347; T. Barnes, A. E. Jacobs, M. D. Kovarik, and W. G. Macready, Phys. Rev. B **45** (1992) 256.
 [38] V. Emery, and S. A. Kivelson, Nature **374** (1995) 4347.
 [39] P. W. Anderson, private communication.